2025 IEEE/SICE International Symposium on System Integration (SII)
January 21-24, 2025, Munich, Germany

Comparison of communication characteristics for local 5G semi-synchronous mode for multiple robot control

Souma Kawanishi[1], Nobuhiko Miyamoto[1], Koji Yoshida[1] and Kazuyoshi Wada[1]

***Abstract*— 5G communications have evolved dramatically and are being used for various purposes. Among them, private communication is expected to be suitable for remote control of multiple robots due to features such as eMBB and mMTC among local 5G. In robot interconnection communication, the emphasis is on the time ratio of uplink communication from each node to the server, while general 5G communication focuses on the time ratio of downlink communication, and the time ratio of uplink communication is small, making it difficult to use for multiple robot control. In this paper, experiments were conducted to improve the uplink eMBB and URLLC by allocating more time resources to the uplink, assuming the advantage of semi-synchronous mode in the TDD communication scheme. The experimental environment was justified by comparing the experimental data with the base station logs. The results showed that not only the throughput of the semi-synchronous uplink was improved, but also the throughput of the TCP downlink.**

I. INTRODUCTION

In recent years, 5G communications have achieved a dramatic technological evolution in wireless network communications and are being used in a variety of situations. Compared to its predecessor, 4G communications, 5G has the following advantages.

- enhanced Mobile Broadband(eMBB)
- Ultra-Reliable and Low Latency Communications(URLLC)
- massive Machine Type Communication(mMTC)

Local 5G (hereafter referred to as L5G), where a dedicated 5G network is built in a specific location, is less susceptible to radio interference due to its planning function. In addition, there are cases where L5G has dedicated frequency bands. Therefore, radio interference such as Wi-Fi and airborne radar can be avoided, and in mobile communications, the handover function enables reliable communication over a wide area[1].

There are examples of networks using Wi-Fi as one of the wireless communication methods to link robots, such as micro logistics platforms[2][3]. However, the 2.4 GHz Wi-Fi band is an ISM band, making it difficult to avoid interference with microwave ovens and BlueTooth. In addition, the 5 GHz band in Japan has mandatory Listen before TalK and DFS features, and there are concerns that these may interfere with the high-speed, low-latency communications required by platforms such as sensor networks[4][5].

*This research was supported by TMU local 5G research support

[1]S.Kawanishi, K.Wada, N.Miyamoto and K.Yoshida are with Graduate School of Systems Design, Tokyo Metropolitan University, 6-6 Asahigaoka, Hino, Tokyo, Japan. k_wada@tmu.ac.jp

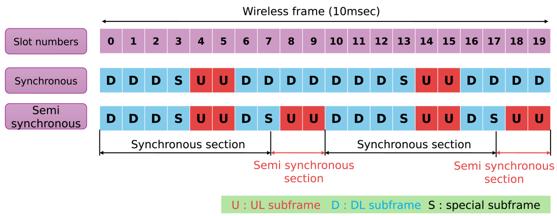

Fig. 1: Radio frame configuration for synchronous/semi-synchronous mode TDD systems

Due to these characteristics, 5G communications have been used to develop systems in various research institutes. Yang et al. describe how 5G networks can optimize vehicle-to-vehicle or vehicle-to-infrastructure communications to enable automated driving and smart cities[6]. Guo et al. show how 5G's fast and secure communications can be used for interhospital collaboration, telemedicine, and real-time patient consultations[7]. Sarah et al. also show how 5G and multi-access edge computing can be combined to achieve end-to-end low latency and high reliability[8]. Damigos et al. show that advanced control can be achieved by using 5G networks to offload control operations from edge servers to enable autonomous operations such as UAVs[9].

In robot networking, client robots upload sensor data from cameras and LiDARs to the server, which in turn sends relatively small amounts of data, such as control commands, to the client. Therefore, the wireless network in robot remote control requires a higher uplink(UL) time ratio than the downlink(DL). However, public wireless communication networks generally focus on the DL communication time ratio and allocate less time to UL communication. Therefore, eMBB and URLLC for UL communication are less likely to be ensured than those for DL communication.

To improve the throughput of uplink communications such as robotics, MediaTec Inc. describes a method to dynamically share transmit power between LTE and 5G NR to increase uplink throughput by increasing the transmit power of the terminal[10].

To solve this problem, semi-synchronous mode in the Time Division Duplex (TDD) scheme has also been proposed in L5G[11][12]. In the L5G frequency band used in this paper, TDD, which uses the same bandwidth for UL and DL and switches the UL and DL slots in detail, is specified as the duplexing method for bidirectional communication. L5G TDD generally uses synchronous mode, where more DL slots are set and frame timings are aligned to avoid interference with public 5G. In contrast, semi-synchronous

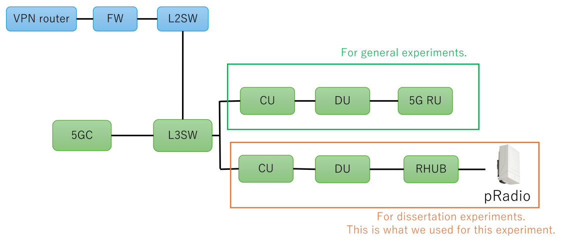

Fig. 2: Equipment configuration diagram of the SUB6 used in the experiment.

TABLE I: Configuration value of the base station at Tokyo Metropolitan University

Item	Set Value
Frequency	4.85GHz
Bandwidth	100MHz
Transmitter power output (eNB)	0.0125W
Antenna Height	3.1m
Time ratio UL:DL	synchronous 2:7 semi synchronous 4:4

TDD, as shown in Fig. 1, synchronizes the start timing of radio frames between base stations, but increases the UL time ratio by changing the UL and DL slots to a segment that does not affect carrier 5G.

To the best of the author's knowledge, there are no cases where the effects of semi-synchronous mode of this TDD system have been measured and the effects on remote control of robots have been investigated. Therefore, this paper compares the communication characteristics before and after the adaptation of semi-synchronous TDD to determine the effects of the introduction of semi-synchronous TDD, and examines its applicability to remote control of robots. In addition, base station protocols such as the MCS index RSRP were obtained and compared with the execution speeds obtained in the experiments to isolate the effects of the external environment.

This paper is structured as follows. Section II describes the actual measurement conditions for local 5G communication characteristics, Section III presents the measurement results for each item. Section IV contains a discussion of the measurement results and, finally, Section V concludes this paper and discusses future research.

II. MEASURING CONDITIONS

A. Measurement Configuration

This paper is based on experiments using L5G installed on the Hino Campus of Tokyo Metropolitan University. Fig. 2 shows the equipment configuration used. There are two systems of CUs, one of which is classified as the dissertation experimental area. In this experiment, this area, including the L5G base station, was measured under occupied conditions. TABLE I shows the configuration values of the L5G sub6 system at Tokyo Metropolitan University.

B. Measurement Environment

The measurement environment is described in this paper. The following measurement equipment was used. However, the router and PC used a commercial power supply to ensure a constant power supply.

- Router：APAL 5G Router RAKU/RAKU Plus[13]
- LAN cable standards：Category5,5e,6,6a,7
- PC：DAIV 5N
  - OS：Ubuntu 20.04
  - Intel Core i7-11800H CPU @ 2.30GHz
  - RAM：32GB

Using the equipment described above, this experiment was conducted in strong and weak electric fields to obtain the change of communication characteristics with the strength of the radio waves. The strong electric field was measured at a distance of about 3 m from the antenna to obtain the maximum MCS index in synchronous TDD operation, and the weak electric field was measured at a distance of about 40 m from the antenna. The measurement position was invariant for both synchronous and semi-synchronous TDD measurements. The RSRP and SIR results are shown in TABLE II.

TABLE II: RSRP and SIR in this experiment

	RSRP[dBm]	SIR[dB]
synchronous/weak	-110 ∼ -130	10 ∼ 30
synchronous/strong	-75 ∼ -80	30 ∼ 40
semi synchronous/weak	-90 ∼ -105	20 ∼ 40
semi synchronous/strong	-65 ∼ -75	25 ∼ 35

C. Measurement Items

This experiment compares the performance of UL and DL communications for synchronous and semi-synchronous modes. In this experiment, throughput for TCP and UDP communications was obtained to confirm the high speed of the network. In addition, the round-trip time (RTT) was obtained to assess the low latency of the network, and the jitter was calculated. Therefore, in this experiment, the following items were measured for 10 seconds for each command, taking into account the time limit to acquire the L5G base station log.

- Throughput
- RTT
- Jitter

TCP throughput was measured using iperf3, and RTT was obtained using ping for a total of 500 times with a time interval of 20 msec. The jitter was measured using mtr, a command that simultaneously obtains network routes and RTT. The configuration values for each experiment are shown in TABLE III. Here 1448 kB is the maximum buffer size that could be written in this experiment. The bandwidth limits were set as shown in TABLE IV. Both were set so that the error rate would be 5-10%. We also collaborated with the L5G base stations to obtain MCS, RB, RSRP, SIR, and CQR to track and measure the correlation between UL and DL throughput and changes in each parameter.

III. RESULT OF EXPERIMENT

First, a comparison of the time series results of throughput by TCP communication is shown in Fig. 3, 4. The graph

TABLE III: Experimental items and their set values

Measurement	Throughput		RTT	Jitter
Setting	Window size [B]	Buffer length [B]	Packet size [B]	Packet size [B]
TCP	Auto, 100, 1k, 10k, 100k	128k	-	100, 1500, 1501, 5k
UDP	-	8k, 1448k	-	100, 1500
ICMP	-	-	5k	100, 1500

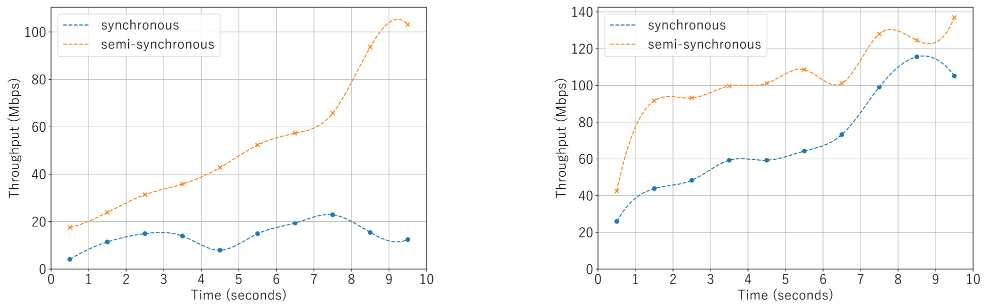

(a) Weak electric field **(b)** Strong electric field

Fig. 3: TCP troughput of UL

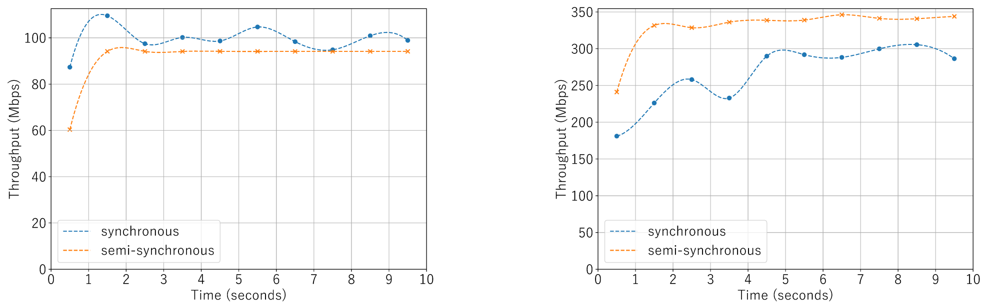

(a) Weak electric field **(b)** Strong electric field

Fig. 4: TCP troughput of DL

TABLE IV: Bandwidth limit for UDP communication in throughput measurement

UL/DL electric field	Synchronous (Mbit/sec)	Semi synchronous (Mbit/sec)
UL weak	90	143
UL strong	200	400
DL weak	950	300
DL strong	950	300

is based on the TCP window size: "auto-set" due to the limitation of base station log collection, and shows the results of throughput collection every second. Although the average throughput value for UL communication in a weak electric field was about 20 Mbps, the average throughput value for semi-synchronous communication was about 60 Mbps, which is an improvement of about three times. However, the throughput value for UL communication in a strong electric field was improved by a factor of 1.5, but the improvement rate was higher in a weak electric field. For DL communication in a strong electric field, the throughput improvement was confirmed by the introduction of semi-synchronization.

Fig. 5, 6 also shows the UL UDP throughput versus MCS index. It can be seen that the TDD synchronous mode keeps the MCS index at 24 and the modulation rate at a high level in a strong electric field. However, the TDD semi-synchronous mode shows a variation in the MCS index, and in the latter half of the time series, the throughput corresponds to the deterioration of the MCS index.

The histograms of the UL and DL RTT resulting from the ping results are shown in Fig. 7-10. The UL RTT was 4ms for the strong electric field and 11ms for the weak electric field, and the worst-case RTT improved for the semi-synchronous TDD compared to the synchronous TDD, but the peak of the normal distribution worsened by 5.6 ms for both the strong and the weak field. The DL RTT showed a deterioration in the worst-case RTT of about 20 ms for the strong electric field and an improvement of about 10 ms for the weak electric field. The peak of the normal distribution remained almost unchanged at around 28 ms. The median and standard deviations for each normal distribution are shown in TABLE V.

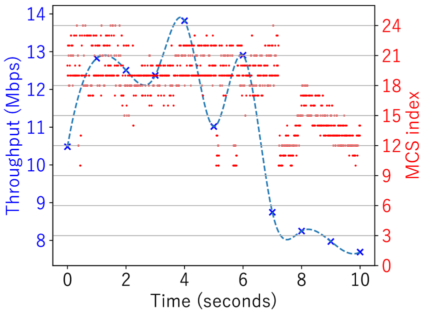

(a) Weak electric field

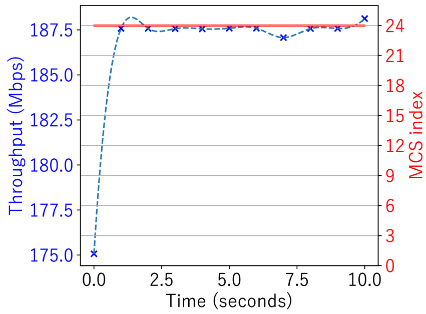

(b) Strong electric field

Fig. 5: Comparison of UL throughput and MCS index for UDP in TDD synchronous mode

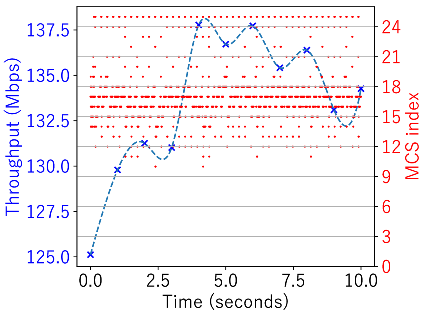

(a) Weak electric field

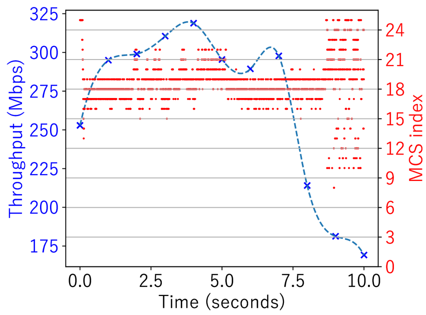

(b) Strong electric field

Fig. 6: Comparison of UL throughput and MCS index for UDP in TDD semi-synchronous mode

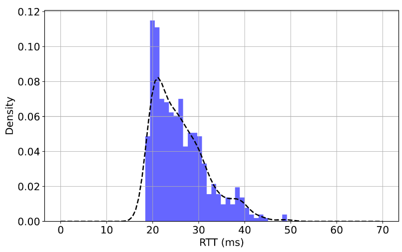

(a) Synchronization

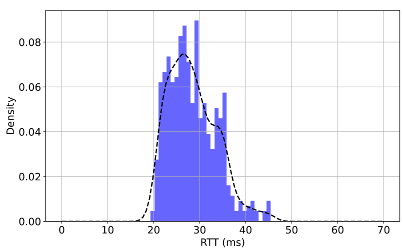

(b) Semi synchronization

Fig. 7: UL RTT in strong electric field

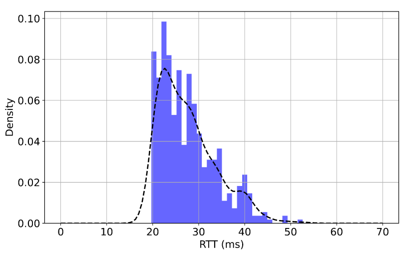

(a) Synchronization

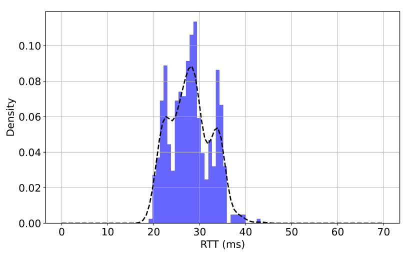

(b) Semi synchronization

Fig. 8: UL RTT in weak electric field

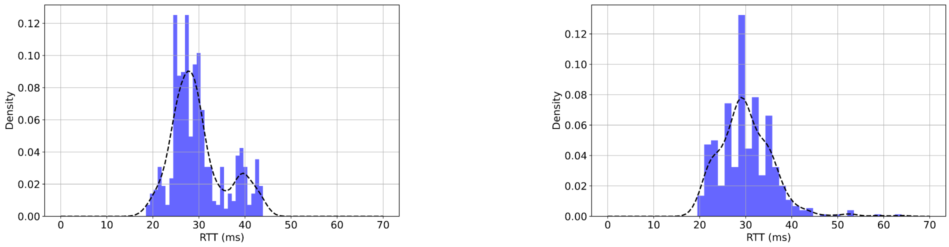

(a) Synchronization **(b)** Semi synchronization

Fig. 9: DL RTT in strong electric field

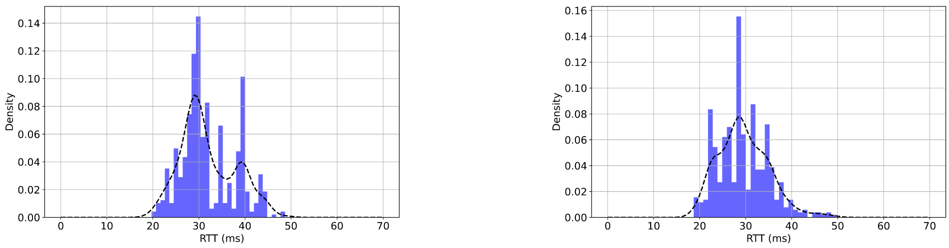

(a) Synchronization **(b)** Semi synchronization

Fig. 10: DL RTT in weak electric field

TABLE V: Median and standard deviation of round trip time

UL/DL electric field	Synchronous (ms)	Semi synchronous (ms)
UL strong	24.9 $\pm$ 5.81	27.6 $\pm$ 5.20
UL weak	26.2 $\pm$ 6.13	28.0 $\pm$ 4.45
DL strong	28.6 $\pm$ 5.78	29.5 $\pm$ 5.80
DL weak	29.8 $\pm$ 5.90	28.8 $\pm$ 5.41

IV. CONSIDERATION

In this paper, we selected a communication protocol that can be adapted to robot remote control, and experimented with the communication characteristics before and after the protocol was adopted. The data to be sent from the robot to the server is assumed to be images, etc. The required wireless communication throughput value is 80 Mbps, assuming that 1 Mbyte images are sent at 0.1 second intervals. Confirming the experimental results, Fig. 3 shows that it is impossible to achieve this TCP throughput value with the weak electric field operation of synchronous TDD, but the introduction of semi-synchronous TDD brings it closer to the target value.

And from Section III, it was the weak electric field that showed the greatest improvement in the UL as a change after the introduction of semi-synchronization. In a strong electric field, an improvement was observed, but the difference was small. In addition, as shown in Fig. 6b, the MCS index remained at 24 in the strong electric field during the synchronous mode of TDD, but the MCS index fluctuated and the throughput decreased during the semi-synchronous mode of TDD. This may be due to the CL-TPC(Closed Loop Transmit Power Control) function installed after the introduction of semi-synchronous mode, which is based on the transmit power control command(TPC) received by the client side from the base station. The CL-TPC function reduces power consumption and unwanted radio wave output and suppresses interference with other communication devices. However, the MCS index decreased due to the transmission power control, and the code rate of the first-order modulation, Quadrature Amplitude Modulation (QAM), was assumed to decrease accordingly. Specifically, Fig. 5,6 show that in synchronous operation the MCS index was stable at 24 and the code rate remained at 841, but in semi-synchronous operation the MCS index varied between 10 and 24 and the code rate fluctuated between 466 and 841. The average code rate was therefore around 650, which would have reduced throughput by around 23%[14]. On the other hand, in weak fields, the CL-TPC function was unaffected and uplink throughput was considered to have improved as expected.

Despite the decrease in the DL time ratio due to the introduction of semi-synchronous TDD, the DL throughput in the strong electric field of TCP communication improved. This is attributed to the reduction of the UL slot interval from 10 to 5 ms, which reduces the response delay of the TCP communication and improves the throughput of the DL communication.

Fig. 7-10 shows that there was an improvement in the worst-case UL RTT in both weak and strong electric fields, and an improvement in the DL in weak electric fields. This is thought to be due to the shortening of the UL slot interval as mentioned earlier.

V. CONCLUSION

In this paper, we improved the UL communication by switching from synchronous TDD to semi-synchronous TDD in L5G and show its communication characteristics. As a result, although the UL TCP throughput was improved regardless of the radio wave strength, the CL-TPC function controlled the transmission power, and the MCS index was degraded even in the strong electric field measurements. We also confirmed that the throughput corresponded to the degradation of the MCS index. In the TCP DL in the strong electric field, the shortened up-slot interval is considered to have improved the throughput despite the small time slot allocation. In the experiments presented in this paper, each measurement was taken for 10 seconds due to the time constraints of logging, but longer measurement times may provide more reproducible results that account for variation.

In this experiment, we confirmed the advantages of eMBB and URLLC in semi-synchronous mode. In future research, we plan to confirm the superiority of the third feature of 5G: mMTC.

ACKNOWLEDGMENT

This research was supported by TMU local 5G research support.

REFERENCES

[1] Amiraslan Haghrah, Mehran Pourmohammad Abdollahi, Hosein Azarhava, and Javad Musevi Niya. "A survey on the handover management in 5G-NR cellular networks: aspects, approaches and challenges". In: *EURASIP Journal on Wireless Communications and Networking* 2023.1 (2023), p. 52.

[2] Efim Poberezkin, Hamid Roozbahani, Marjan Alizadeh, and Heikki Handroos. "Development of a robust Wi-Fi/4G-based ROS communication platform for an assembly and repair mobile robot with reliable behavior under unstable network or connection failure". In: *Artificial Life and Robotics* 27.4 (2022), pp. 786–795.

[3] Xuxin Lin, Jianwen Gan, Chaohao Jiang, Shuai Xue, and Yanyan Liang. "Wi-Fi-Based Indoor Localization and Navigation: A Robot-Aided Hybrid Deep Learning Approach". In: *Sensors* 23.14 (2023), p. 6320.

[4] Isidro Calvo, Oscar Barambones, Ander Chouza, Steven Abrahams, Geert Beckers, Dieter Slechten, and Javier Velasco. "Building wireless control applications with XBee and LabVIEW". In: *Applied Sciences* 9.11 (2019), p. 2379.

[5] Edward J Oughton, William Lehr, Konstantinos Katsaros, Ioannis Selinis, Dean Bubley, and Julius Kusuma. "Revisiting wireless internet connectivity: 5G vs Wi-Fi 6". In: *Telecommunications Policy* 45.5 (2021), p. 102127.

[6] Yang Yang and Kun Hua. "Emerging technologies for 5G-enabled vehicular networks". In: *IEEE access* 7 (2019), pp. 181117–181141.

[7] Caixia Guo and Hong Li. "Application of 5G network combined with AI robots in personalized nursing in China: A literature review". In: *Frontiers in Public Health* 10 (2022), p. 948303.

[8] Annisa Sarah, Gianfranco Nencioni, and Md. Muhidul I. Khan. "Resource Allocation in Multi-access Edge Computing for 5G-and-beyond networks". In: *Computer Networks* 227 (2023), p. 109720. ISSN: 1389-1286. DOI: `https://doi.org/10.1016/j.comnet.2023.109720`.

[9] Gerasimos Damigos, Tore Lindgren, and George Nikolakopoulos. "Toward 5g edge computing for enabling autonomous aerial vehicles". In: *IEEE Access* 11 (2023), pp. 3926–3941.

[10] MediaTek Inc. *5G NR Uplink Enhancements: Better Cell Coverage & User Experience*. 2018. URL: `https://newsletter.mediatek.com/hubfs/mwc/download/ul-enhancements.pdf` (visited on 11/06/2024).

[11] "Dynamic adjustment of downlink / uplink allocation ratio and signaling method in LTE / TDD system". JP2011521500A. Aug. 2011.

[12] Ministry of Internal Affairs and Communications. '*Technical conditions for local 5G maritime use, etc.*' *in* '*Technical conditions for new generation mobile communication systems*'. (Visited on 11/26/2024).

[13] *5G Qualcomm X55 Mifi, APAL*. URL: `https://www.apaltec.com/mifi/` (visited on 08/06/2024).

[14] ShareTechnote. *5G/NR - MCS/TBS/Code Rate*. `https://www.sharetechnote.com/html/5G/5G_MCS_TBS_CodeRate.html`. (Visited on 11/26/2024).